Performance of the solid state neutral particle analyzer array on the national spherical torus experiment

D. Liu and W. W. Heidbrink
University of California at Irvine, Irvine, California 92697

D. S. Darrow, A. L. Roquemore, and S. S. Medley
Princeton Plasma Physics Laboratory, Princeton, New Jersey 08543

K. Shinohara
Japan Atomic Energy Agency, Naka, Ibaraki 311-0193, Japan

(Received 8 May 2006; presented on 10 May 2006; accepted 13 June 2006; published online 2 October 2006)

The solid state neutral particle analyzer (SSNPA) array on the national spherical torus experiment (NSTX) consists of four chords with tangency radii of 60, 90, 100, and 120 cm that view across the three coinjection neutral beam lines. Each chord utilizes a silicon photodiode that is coupled to fast digitizers to measure the energy distribution of charge exchange fast neutral particles (30–100 keV). By the end of the NSTX 2005 experimental campaign, the electromagnetic noise in the SSNPA was reduced by half and reasonable signals were obtained with good electromagnetic shielding, fast digitization of raw signals, software-based pulse height analysis, and pulse shape discrimination. Energy resolution of ~10 keV and time resolution of 2 ms have been achieved. Temporal evolutions of energetic neutral flux obtained with the SSNPA are in good agreement with those obtained with the $E \| B$-type neutral particle analyzer. With these improvements, the SSNPA can be used to study magnetohydrodynamic instabilities and fast ion redistribution. Example data from plasma discharges are presented along with the noise reduction techniques and postshot pulse height analysis methods. © *2006 American Institute of Physics.* [DOI: 10.1063/1.2227440]

I. INTRODUCTION

The neutral particle analyzer (NPA) is a well-established diagnostic used to measure the energy distribution of charge exchange neutral particles escaping from plasmas to deduce the fast ion energy and spatial distribution inside the plasmas. Such information is important for studying fast ion confinement and transport mechanisms both in quiescent plasmas and in the presence of magnetohydrodynamic (MHD) activity. The conventional "*E*-parallel-to-*B*" ($E \| B$)-type NPA (Ref. 1) uses a stripping cell to reionize the neutrals and electric and magnetic fields to deflect the particles onto a microchannel plate detector. But the significant size and cost of this diagnostic make it difficult to build a multichannel system. Recently, compact semiconductor detectors[2] (natural diamond detectors and silicon diodes) have been proposed as an alternative way of measuring the energy of charge exchange neutrals and have been tested on several magnetic fusion experiments.[3–8] When a neutral particle impacts a semiconductor detector, it produces a pulse of electron-hole pairs that is converted to a voltage pulse by a charge sensitive preamplifier and amplified by a second stage amplifier. The final pulse height is linearly related to the incident particle energy. In this way, the energy spectrum of the escaping neutral particles can be obtained through analog circuits or digital pulse height analysis. Since the silicon diode has higher carrier collection efficiency and lower cost than diamond, a prototype of the solid state neutral particle analyzer (SSNPA) array[9] which utilizes silicon photodiode detectors was installed on the national spherical torus experiment (NSTX) in 2004. Several layers of electromagnetic (EM) shielding were provided for the detectors and flight tubes, but the SSNPA array still picked up large EM noise. Also, the second stage amplifier has a single-ended input that requires a very quiet ground, which is not the case for NSTX. Due to the above reasons, the SSNPA energy spectrum was contaminated making it difficult to get useful or detailed information from the measured energy spectrum. In this article, noise reduction techniques for the SSNPA and a software-based pulse height analysis method are described. Initial measurement results of fast neutral particle profiles on NSTX are shown in Sec. IV.

II. EXPERIMENTAL SETUP

A. Electromagnetic shielding

The SSNPA array on NSTX consists of four chords with tangency radii of 60, 90, 100, and 120 cm viewing across the three coinjection neutral beam lines. The layout of the SSNPA and a diagram of original electronic circuits are shown in Figs. 3 and 4 of Ref. 9. The electronics before the second stage amplifier, including the detector, the preamplifier, and a long signal cable are most sensitive to EM pickup since they are very close to strong magnetic fields from the toroidal and poloidal coils (10 cm from the toroidal field coils and 50 cm from the poloidal field coils), and any EM pickup will be amplified by the second stage amplifier. Several improvements were made in the NSTX 2005 experimental campaign:

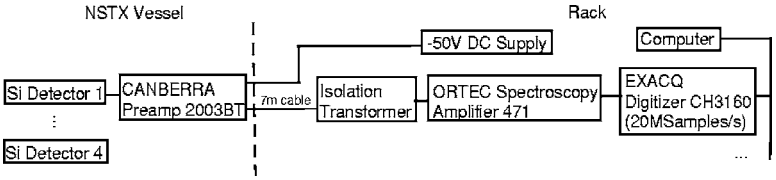

FIG. 1. Schematic diagram of the SSNPA electronics.

(1) low capacitance and low dark current AXUVHS5 detectors[10] were carefully selected since they will finally determine the energy resolution and low-energy limit of the measurable energy range; (2) the position of the preamplifiers was rearranged so that each preamplifier was attached to the detector directly without any cable so no additional capacitance was added to the preamplifier input side; (3) preamplifiers and connectors were shielded in a copper box that was grounded to the instrument rack; (4) the cables between the preamplifier and the amplifier were shortened from 10 to 7 m and the coaxial signal cable was replaced by a shielded twisted-pair cable; (5) the cables for one chord that consist of one bundle were gently twisted and covered with a grounded braid and magnetic shielding foil (METGLAS 2605CO);[11] and (6) the four bundles were put in an aluminum conduit which was also grounded to the instrument rack and a wide bandwidth transformer was inserted in series with the signal cable to eliminate possible ground loops. With these improvements, the detector, preamplifier and cables have good EM shielding that significantly reduced the noise pickup in plasma discharges. The block diagram of the revised SSNPA setup is shown in Fig. 1. A charge sensitive preamplifier (CANBERRA 2003BT) with a sensitivity of 20 mV/MeV, a fast shaping amplifier (ORTEC 471) with shaping time 0.5 μs, and two digitizer boards (that will be described below) are used in the current SSNPA array design.

B. Fast digitization of raw signals

In the NSTX 2005 experimental campaign, the conventional analog pulse height analysis module of the SSNPA was replaced by a digital pulse height and shape analysis system. The output signal of the second stage amplifier was directly connected to a PCI digitizer board (EXACQ CH3160),[12] with an onboard memory of 64 Mbytes. The digitizer board provides either one input channel with a sampling rate at 40 MHz, two input channels at 20 MHz, or four input channels at 10 MHz. Input signals up to ±5 V can be fed and the energy resolution is 12 bits. Standard transistor-transistor logic (TTL) signals are used for triggering. Currently two digitizer boards are used at a 20 MHz sample rate for two channels on each board. Data is sampled continuously after a start trigger until either a preset time arrives or the onboard memory is full. Afterwards, the data are transferred to a local programable computer. Dedicated LABVIEW and IDL programs were developed for data acquisition and analysis, respectively. This novel digital approach provides several important features: accurate pulse height measurement, pulse shape discrimination, post experiment data reprocessing, pulse pileup identification and treatment, and possible high count rate operation. In addition, this digitization method is also very useful in resolving noise sources. Through this digitization method, it was found that the EM noise had a fixed frequency related to the coil system used for resistive wall mode control.[13]

III. SOFTWARE-BASED PULSE HEIGHT ANALYSIS

The software-based pulse height analysis consists of several stages: (a) filtering to remove low frequency noise and smooth the raw data; (b) rejection of pulses below a preset threshold; (c) peak location for pairs of adjacent overlapping pulses that exceed the threshold; and (d) determination of the base line, peak position, peak value, and pulse width for individual pulses. The pulse height equals the peak value minus the base line, and each pulse is normalized to its pulse height and compared with the model pulse shape. If the reduced chi squared is smaller than a specified value which means that the measured pulse shape is very similar to the pulse model, that pulse is accepted as a true signal pulse. Otherwise, the pulse is rejected as EM noise. In contrast to conventional analog pulse height analysis (PHA), this digitization method, in principle, also enables the disentanglement of two overlapping pulses and determination of the pulse height for both pulses.[14] If any pulse width is larger than a certain maximum value, it is considered a possible pulse pileup event. In such cases, the first signal is fitted up to the start of the second one. The analytical function obtained from the fit is subtracted, thus isolating the second pulse, which can then be separately analyzed. But this reconstruction still requires a minimum fit interval between two pulses in order to obtain stable results for the first pulse. An example of this digitization method is shown in Fig. 2 with (a) the raw signals with true peaks marked with a plus and noise marked with a diamond; (b) the pulse shape comparison of the true signals (solid blue curve) with the pulse model (bold red curve); and (c) the pulse shape comparison of noise (solid blue curves) with the pulse model (bold red curve). With this digitization method, pulse height is accurately measured and obvious noise pulses due to EM pickup are rejected. However, the ideal arrangement for the digitization method is to sample the raw signals after the preamplifiers.[15] Unfortunately, the available preamplifiers do not have sufficient gain (the output signals are only the order of a millivolt).

IV. EXPERIMENTAL RESULTS ON NSTX AND DISCUSSION

During calibration of the motional Stark effect diagnostic, neutral beams (NB) are injected into the NSTX vessel without a target plasma in what is referred to as gas-filled-torus shots. In these shots, some of the NB-injected particles are ionized by collisions with the residual gas and captured on the toroidal magnetic field lines. The electron density is

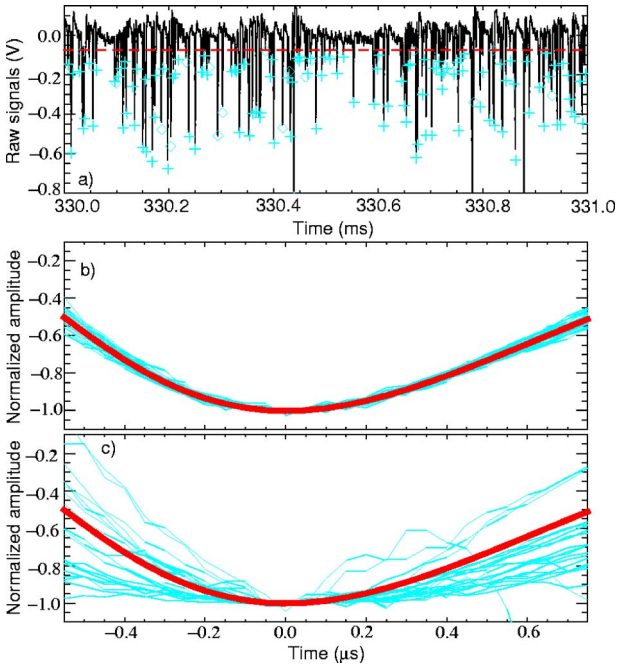

FIG. 2. (a) (Color online) Raw data for chord 1 of the SSNPA with true signals marked with plus and noise marked with diamond; (b) pulse shape comparison of the true signals (solid blue curves) with the pulse model (bold red curve); and (c) pulse shape comparison of noise (solid blue curves) with the pulse model (bold red curve).

very low, hence the slowing-down time is long and particle loss by charge exchange is significant. Therefore, the spectra obtained on a sight line close to the tangency radius of the injected NB should be the same as the injected neutral energy spectra. This can be used for energy calibration[6] or validity checking of the SSNPA performance. The solid black curve in Fig. 3 shows a typical measured energy spectrum obtained on chord 1 of the SSNPA in the gas-filled-torus shot 118186 in which NB source A was injected at 90 keV. Full and half energy components of the injected NB (deuterium) are clearly seen and an energy resolution of 10 keV is achieved.

From the measured energy spectrum, a high-energy tail

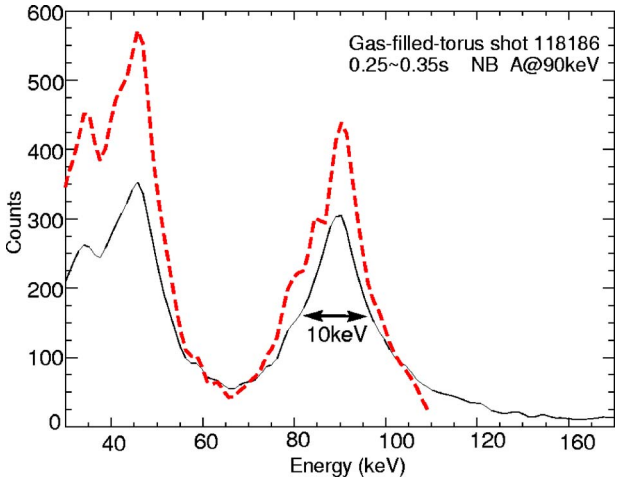

FIG. 3. (Color online) Measured energy spectrum (solid black curve) for chord 1 of the SSNPA in a gas-filled shot and the true energy spectrum (dashed red curve) inversely derived through Monte Carlo simulation.

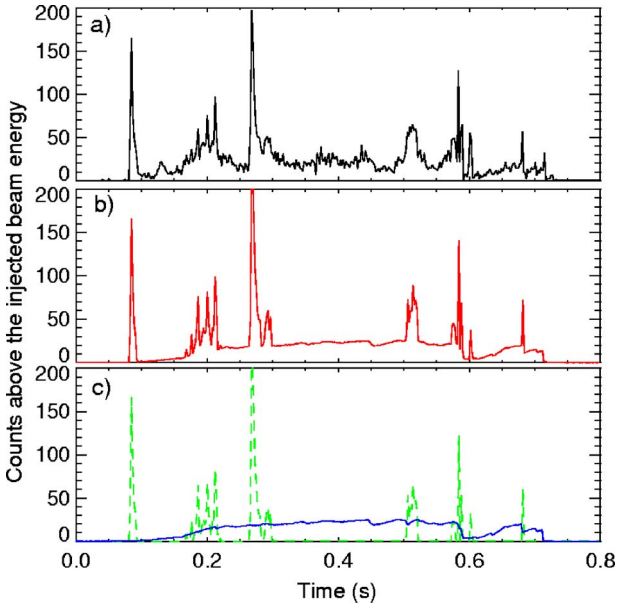

FIG. 4. (a) (Color online) Temporal evolution of counts above the injected beam energy; (b) the empirical linear combination of pulse pileup and neutron/gamma radiation; and (c) contribution of pulse pileup (dashed green curve) and neutron/gamma radiation (solid blue curve).

above the injected beam energy is also observed. Since there is no plasma in gas-filled-torus shots and hence no neutron/gamma radiation, the high-energy tail can only be caused by unentangled pulse pileup. A Monte Carlo code[16] can be used to simulate pulse pileup trains if the true count rate and spectrum are available. In our case, the true count rate can be obtained by numerical inversion from the paralyzable model[17] and the measured energy spectrum can be used as the initial estimate of the true spectrum. With iteration, the true energy spectrum can be inversely derived from the uncorrected experimental spectra. The dashed red curve in Fig. 3 shows the derived true energy spectrum. It is clearly seen that pileup will generate the high-energy tail, but this does not significantly distort the spectral shape below the injection energy. The examination of a number of discharges indicates that the fraction of pulses above the injection energy increases monotonically with count rate. Eight reproducible gas-filled-torus shots were chosen to estimate the coefficient between the pulse counts above the beam injected energy and the total neutral flux incident on the detector. Also, several shots with the closed SSNPA valve were used to eliminate the neutral flux onto the detectors and to estimate the neutron/gamma contribution to the SSNPA signals. As shown in Fig. 4, the empirical linear combination [red curve in Fig. 4(b)] of pulse pileup [solid blue curve in Fig. 4(c)] and neutron radiation [dashed green curve in Fig. 4(c)] is in good agreement with the experimental pulse count evolution above the injected beam energy [solid black curve in Fig. 4(a)] which suggests that the high-energy tail is due to the combined effects of pulse pileup and background signal from neutron/gamma radiation.

Figure 5 shows the temporal evolution of plasma current, injected NB power, neutron yield, 80 keV neutral flux measured by the $E\|B$-type NPA (with tangency radius of 63.5 cm), and chord 1 of the SSNPA (with tangency radius

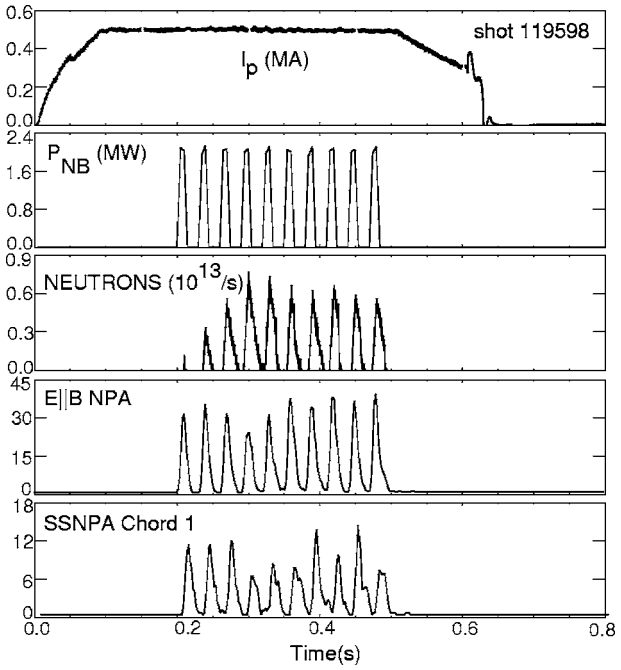

FIG. 5. Temporal evolution of plasma current I_p, NB power, neutron yield, counts in chord 1 of the SSNPA (tangency radius of 60 cm), and the $E\|B$ NPA signal (tangency radius of 63.5 cm).

of 60 cm). The NB (source A) blips are injected at a full energy of 90 keV with 10 ms on and 20 ms off. The signals of SSNPA chord 1 are clearly synchronized to the modulation of the NB and the temporal evolution is similar to that obtained with the $E\|B$-NPA. During the NB off period, the slowing down of the beam ions is observed.

The maximum count rate of the present system is around 200 kc/s, which is mainly limited by the second stage amplifier. An ultrafast amplifier will increase the time resolution and improve the counting statistics. Cooling the detector and preamplifier can reduce detector leak current and increase SSNPA energy resolution, but this is left for future work.

ACKNOWLEDGMENTS

The authors would like to acknowledge Tom Holoman and Doug LaBrie for their helpful technical assistance. This work was supported at PPPL by DOE Contract No. DE-AC02-76CH03073.

[1] S. S. Medley and A. L. Roquemore, Rev. Sci. Instrum. **69**, 2651 (1998).
[2] A. V. Krasilnikov, V. N. Amosov, and Yu. A. Kaschuck, IEEE Trans. Nucl. Sci. **45**, 385 (1998).
[3] A. V. Krasilnikov S. S. Medley, N. N. Gorelenkov, R. V. Budny, O. V. Ignatyev, Yu A. Kaschuck, M. P. Petrov, and A. L. Roquemore, Rev. Sci. Instrum. **70**, 1107 (1999).
[4] M. Isobe *et al.*, Rev. Sci. Instrum. **72**, 611 (2001).
[5] T. Yamamoto *et al.*, Rev. Sci. Instrum. **72**, 615 (2001).
[6] M. Osakabe *et al.*, Rev. Sci. Instrum. **72**, 788 (2001).
[7] A. G. Alekseyev, D. S. Darrow, A. L. Roquemore, S. S. Medley, V. N. Amosov, A. V. Krasilnikov, D. V. Prosvirin, and A. Yu. Tsutskikh, Rev. Sci. Instrum. **74**, 1905 (2003).
[8] J. F. Lyon, P. R. Goncharov, S. Murakami, T. Ozaki, D. E. Greenwood, D. A. Spong, and S. Sudo, Rev. Sci. Instrum. **74**, 1873 (2003).
[9] K. Shinohara, D. S. Darrow, A. L. Roquemore, S. S. Medley, and F. E. Cecil, Rev. Sci. Instrum. **75**, 3640 (2004).
[10] http://www.ird-inc. com/axuvhigh. html
[11] http://www.metglas.com/jp/products/page5_1_2_1.htm
[12] http://www.exacqdaq. com/ch3160_specs.html
[13] S. A. Sabbagh *et al.*, Nucl. Fusion **46**, 635 (2006).
[14] S. Marrone *et al.*, Nucl. Instrum. Methods Phys. Res. A **490**, 299 (2002).
[15] P. R. Goncharov *et al.*, Rev. Sci. Instrum. **75**, 3613 (2004).
[16] W. Guo, S. H. Lee, and R. P. Gardner, Nucl. Instrum. Methods Phys. Res. A **531**, 520 (2004).
[17] G. F. Knoll, *Radiation Detection and Measurement*, 3rd ed. (Wiley, New York, 2000).